Received: 25 April 2018 | Accepted: 25 June 2018

DOI: 10.1111/cas.13713

ORIGINAL ARTICLE

WILEY Cancer Science

Changes in plasma membrane damage inducing cell death after treatment with near-infrared photoimmunotherapy

Kohei Nakajima[1] | Hideo Takakura[1] | Yoichi Shimizu[1] | Mikako Ogawa[1,2]

[1]Laboratory of Bioanalysis and Molecular Imaging, Graduate School of Pharmaceutical Sciences, Hokkaido University, Sapporo, Japan

[2]PRESTO, Japan Science and Technology Agency, Kawaguchi, Japan

Correspondence: Mikako Ogawa, Laboratory of Bioanalysis and Molecular Imaging, Graduate School of Pharmaceutical Sciences, Hokkaido University, Sapporo, Japan (mogawa@pharm.hokudai.ac.jp).

Funding information
Astellas Foundation for Research on Metabolic Disorders; Terumo Foundation for Life Sciences and Arts; Precursory Research for Embryonic Science and Technology, Grant/Award Number: JPMJPR15P5; JSPS KAKENHI, Grant/Award Number: 16H05382, 16K15568

Near-infrared photoimmunotherapy (NIR-PIT) is a new cancer phototherapy modality using an antibody conjugated to a photosensitizer, IRDye700DX. When the conjugate binds to the plasma membrane and is exposed to NIR light, NIR-PIT-treated cells undergo swelling, and target-selective necrotic/immunogenic cell death is induced. However, the cytotoxic mechanism of NIR-PIT has not been elucidated. In order to understand the mechanism, it is important to elucidate how the damage to the plasma membrane induced by NIR light irradiation changes over time. Thus, in the present study, we investigated the changes in plasma membrane permeability using ions and molecules of various sizes. Na^+ flowed into cells immediately after NIR light irradiation, even when the function of transporters or channels was blocked. Subsequently, fluorescent molecules larger than Na^+ entered the cells, but the damage was not large enough for dextran to pass through at early time points. To assess these phenomena quantitatively, membrane permeability was estimated using radiolabeled ions and molecules: $^{111}InCl_3$, ^{111}In-DTPA, and ^3H-H_2O, and comparable results were obtained. Although minute plasma membrane perforations usually do not induce cell death, our results suggest that the minute damage induced by NIR-PIT was irreversibly extended with time. In conclusion, minute plasma membrane damage is a trigger for the increase in plasma membrane permeability, cell swelling, and necrotic/immunogenic cell death in NIR-PIT. Our findings provide new insight into the cytotoxic mechanism of NIR-PIT.

KEYWORDS
cell membrane damage, immunogenic cell death, near-infrared photoimmunotherapy, photosensitizer, phototherapy

1 | INTRODUCTION

Near-infrared photoimmunotherapy (NIR-PIT) is a newly developed cancer therapy using antibody-photosensitizer conjugates followed by NIR light exposure. The highly hydrophilic silicon-phthalocyanine derivative, IRDye700DX (IR700), is used as a photosensitizer.[1] A clinical trial using cetuximab-IR700 conjugates (anti-human epidermal growth factor receptor type-1) in patients with recurrent head and neck cancer has been approved in 2015 by the US Food and Drug Administration, and the phase I/II study was finished with good success in 2017 (https://clinicaltrials.gov/ct2/show/NCT02422979). When a monoclonal antibody-IR700 conjugate (mAb-IR700) binds to an antigen on the target cell membrane and is exposed to NIR light, selective cytotoxic effects are induced. Cells treated with NIR-PIT eventually develop blebs, resulting in cell death.

Necrotic cell death and apoptotic cell death are two major processes of cell death, and the plasma membrane damage induced by NIR-PIT is necrotic rather than apoptotic.[2] The cytotoxicity of photodynamic therapy (PDT), conventional phototherapy, is mainly related to reactive oxygen species (ROS) generated from excited

photosensitizers. Apoptosis is a general major cell death process in PDT.[3,4] In contrast, NIR-PIT induces cell death under hypoxic conditions, the cells are killed in the presence of ROS scavengers, and caspase-3 activity is not increased.[1,5,6] Thus, apoptotic cell death is not the main mechanism of cell death in NIR-PIT, and necrotic/immunogenic cell death is induced.[7]

In previous studies on necrotic/immunogenic cell death, obvious morphological changes such as cell swelling and bleb formation were observed in NIR-PIT-treated cells.[1,7,8] Plasma membrane-targeted photosensitizers for PDT induce plasma membrane damage by ROS and blebs are also formed.[9,10] In contrast, several studies have shown that ROS is not the factor responsible for inducing membrane damage in NIR-PIT.[1,5,11,12] Thus, in order to understand the cytotoxic mechanism of NIR-PIT, it is important to elucidate how the damaged plasma membrane changes during the process of cell swelling and bleb formation. Therefore, in the present study, we aimed to investigate the changes in plasma membrane damage at early time points during NIR-PIT. The severity of plasma membrane damage was evaluated by permeability changes for various sizes of ions and molecules. Our findings on the plasma membrane damage will provide new insight into the cytotoxic mechanism of NIR-PIT.

2 | MATERIALS AND METHODS

2.1 | Reagents

Trastuzumab (Herceptin®), 95% humanized IgG1 mAb against the extracellular domain of the human epidermal growth factor receptor type-2 (HER2), was purchased from Chugai Pharmaceutical Co., Ltd (Tokyo, Japan). The silicon-phthalocyanine derivative, IRDye700DX NHS ester (IR700), was purchased from Li-COR Bioscience (Lincoln, NE, USA). All the other chemicals used were of reagent grade.

2.2 | Synthesis of IR700 conjugated antibodies

Trastuzumab (1 mg, 6.8 nmol) was incubated with IR700 (66.8 μg, 34.2 nmol) in 0.1 mol/L Na_2HPO_4 (pH 8.5) at room temperature for 2 hours. The reaction mixture was purified on a Sephadex G25 column (PD-10; GE Healthcare, Milwaukee, WI, USA) to derive trastuzumab-IR700 (Tra-IR700). Protein concentrations were determined with the Modified Lowry Protein Assay Kit (Thermo Fisher Scientific Inc., Rockford, IL, USA) by measurement of light absorption at 750 nm with the Infinite M200 instrument (Tecan Austria GmbH, Grödig, Austria). Concentration of IR700 was measured by absorption at 689 nm with a spectrometer (UV-1800; Shimadzu Corp., Kyoto, Japan) in order to determine the number of IR700 molecules conjugated to each mAb molecule: approximately 3 IR700 molecules were bound to a single mAb.

2.3 | Cell culture

HER2-gene-transfected NIH3T3 (3T3-HER2) cells were a gift from Dr Hisataka Kobayashi (Molecular Imaging Program, Center for Cancer Research, National Cancer Institute, NIH, Bethesda, USA). Cells were grown in RPMI-1640 (Sigma, St Louis, MO, USA) containing 10% FBS (Gibco Life Technologies, Grand Island, NY, USA) and 1% penicillin/streptomycin (Nacalai Tesque, Kyoto, Japan) in tissue culture dishes in a humidified incubator at 37°C in an atmosphere of 95% air and 5% carbon dioxide.

2.4 | Observation of ion flow-in

The Na^+-sensitive fluorescent reagent, CoroNa Green-AM (Molecular Probes, Eugene, OR, USA), was used to observe intracellular concentration changes of Na^+ after NIR light irradiation. CoroNa Green-AM enters cells and, after hydrolysis (MW 564.54 after hydrolysis), depending on the Na^+ concentration, it produces a green fluorescence.[13] 3T3-HER2 cells were seeded on culture dishes and incubated for 24 hours. Tra-IR700 (5 μg/mL) was added to the culture medium and the cells were incubated for 55 minutes at 37°C. After incubation, CoroNa Green-AM was added to the medium (2 μmol/L), and the cells were incubated for 5 minutes. Then, the medium was changed to fresh medium or 2 different high osmotic pressure media after washing the cells with PBS. The media were prepared by adding 25 mmol/L NaCl or 50 mmol/L dextran (MW ~6000; Sigma) to RPMI-1640. Immediately after replacing medium, changes in fluorescent intensity were observed using a fluorescent microscope (CKX41; Olympus Corporation, Tokyo, Japan). A filter set to detect fluorescence of CoroNa Green consisted of a 460-490-nm excitation filter and a 520-nm long-pass emission filter. The cells were irradiated with NIR light (2 J/cm^2) using a light-emitting diode (LED) emitting light at 670-710 nm (L690D-66-16100; Epitex Inc., Kyoto, Japan). Power density was measured with an optical power meter (PM100; Thorlabs, Newton, NJ, USA; 50 mW/cm^2). To inhibit the function of Na^+ transporters or voltage-dependent sodium channels, the experiments were also carried out at 4°C or in the presence of 1 μmol/L tetrodotoxin (TTX).[14] Image analysis was conducted with ImageJ software (http://rsb.info.nih.gov/ij/).

2.5 | Observation of plasma membrane permeability changes

For assessment of changes in plasma membrane permeability, the LIVE/DEAD Viability/Cytotoxicity Kit (Molecular Probes) was used. This assessment depends on the physical and biochemical properties of cells. Cell-permeable calcein-AM penetrates live-cell membrane due to its lipophilicity and produces an intense green fluorescence after hydrolysis (MW 622.55 after hydrolysis). It is retained in cells unless the cells are dead. Ethidium homodimer-1 (EthD-1, MW 865.77) cannot penetrate a live-cell membrane due to its size and charge. After cells are dead, EthD-1 enters cells, where it binds to nucleic acids and is retained. Molecular diameters were calculated by using ChemBioDraw (PerkinElmer, Inc., Boston, MA, USA).[15,16]

3T3-HER2 cells were seeded on culture dishes and incubated for 24 hours. Tra-IR700 (5 μg/mL) was added to the culture medium and incubated for 30 minutes at 37°C, and then LIVE/DEAD reagents were added to the medium. After 30 minutes, the cells were washed

with PBS, and the medium was replaced with fresh culture medium containing LIVE/DEAD reagents. The cells were observed under a fluorescence microscope (CKX41; Olympus Corporation). To detect the fluorescence of calcein, a filter consisting of a 460-490-nm excitation filter and a 520-nm long-pass emission filter was used. A filter set to detect fluorescence of EthD-1 consisted of a 480-550-nm excitation filter and a 590-nm long-pass emission filter. The cells were irradiated with NIR light (2 J/cm^2) using an LED. Image analysis was conducted with ImageJ software (http://rsb.info.nih.gov/ij/).

2.6 | $^{111}InCl_3$, ^{111}In-DTPA, and ^3H-H_2O cell-uptake study

In order to quantify the cell uptake of ions or small molecules after NIR light irradiation $^{111}InCl_3$, ^{111}In-DTPA (Nihon Medi-Physics Co. Ltd., Tokyo, Japan) and ^3H-H_2O (PerkinElmer, Inc.) were used. 3T3-HER2 cells were seeded at 1×10^6 on 35-mm dishes. Cells in the Tra-IR700 (+) group were incubated with Tra-IR700 (5 μg/mL) for 1 hour. After washing with PBS, fresh medium or 2 different high osmotic pressure media containing these radiotracers were added to each dish. The high osmotic pressure media were prepared by adding 25 mmol/L NaCl or 50 mmol/L dextran (MW ~6000) to RPMI-1640. Immediately after adding medium, cells were exposed to NIR light (2 J/cm^2) using the LED. The cells were incubated for 3 minutes or 60 minutes at 37°C after irradiation, and they were then detached from the dishes by incubation with trypsin EDTA. After cell-washing centrifugation with PBS, the cells were lysed in 0.1 N NaOH and radioactivity was measured with an automatic γ-counter (1480 Wizard 3; PerkinElmer, Inc.) or a liquid scintillation counter (LSC-5100; Hitachi-Aloka Medical, Tokyo, Japan). Protein concentration was measured with the BCA protein assay kit (Thermo Fisher Scientific Inc.). The uptake was presented as percentage dose per milligram of protein.

2.7 | Statistical analysis

Data are expressed as means ± SEM from a minimum of 4 experiments. Statistical analyses were carried out using JMP Pro 12.2.0 software (SAS Institute Inc., Cary, NC, USA). For multiple comparisons, a one-way analysis of variance (ANOVA) with the Tukey-Kramer test was used. Differences were considered statistically significant when *P*-values were <.05.

3 | RESULTS

3.1 | NIR-PIT rapidly induced Na^+-inflow, but dextran did not enter cells at early time points

In order to evaluate minute plasma membrane damage, we observed Na^+-inflow after NIR light irradiation by using the Na^+-indicator. The ionic diameter of Na^+ in aqueous solution is about 0.5 nm.[17] The extracellular concentration of Na^+ is approximately 130 mmol/L, and the concentration in cytosol is 5-15 mmol/L.[18] Thus, Na^+ will flow into cells if the plasma membrane damage is larger than the Na^+ diameter. Immediately after NIR light irradiation, the fluorescent intensity of the Na^+-indicator was increased, indicating that Na^+ rapidly entered cells (Figure 1A; Video S1). Na^+ flowed into cells even at 4°C (Figure 1B), and in the presence of TTX immediately after NIR light irradiation (Figure 1C).

Size of plasma membrane damage was evaluated by observing Na^+-inflow under high osmotic pressure conditions, which were established with NaCl or dextran. The diameter of dextran molecules in the experiments was about 3.7 nm.[19] Under high osmotic pressure conditions, Na^+-inflow into cells occurs when the plasma membrane damage is larger than the size of the solute molecules responsible for the osmotic pressure. Figure 2A shows Na^+-inflow under high osmotic pressure condition caused by NaCl. In contrast, Na^+ did not flow into cells under high osmotic pressure conditions established by dextran (Figure 2B). These results suggest that the initial plasma membrane damage induced by NIR-PIT is large enough for Na^+ and Cl^- to pass through, but not large enough for dextran to pass through.

3.2 | Plasma membrane permeability was increased after NIR light irradiation

Changes in plasma membrane permeability after NIR light irradiation were evaluated using 2 different fluorescent molecules, calcein-AM and EthD-1 (Figure 3). The molecular diameters of calcein and EthD-1 were 1.4 and 2.6 nm, respectively. Although calcein did not leak out immediately after NIR light irradiation, it gradually disappeared from the cells at 3 minutes after NIR light irradiation before obvious plasma membrane damage was observed in bright field images. EthD-1 entered cells only after many blebs were observed in bright field. These results suggested that the permeability increased with time after NIR light irradiation when the plasma membrane damage was extensive.

3.3 | $^{111}In^{3+}$ rapidly entered cells immediately after NIR light irradiation

Uptake of ions after NIR light irradiation was quantified with radioisotopes. $^{111}In^{3+}$ was used to investigate the inflow of small ions at 3 and 60 minutes after NIR light exposure and to evaluate plasma membrane damage. The calculated ionic diameter of $^{111}In^{3+}$ in aqueous solution is about 0.4 nm.[17] Uptake studies were also carried out under high osmotic pressure conditions established by NaCl or dextran. As shown in Figure 4A, NIR-PIT-treated cells both in a control medium and in a high osmotic pressure medium established by NaCl allowed inflow of $^{111}In^{3+}$ at both 3 and 60 minutes, with no significant difference in the uptake between these time points. In contrast, in a high osmotic pressure medium established by dextran, $^{111}In^{3+}$-inflow was observed neither at 3 minutes nor at 60 minutes.

3.4 | The small molecule, ^{111}In-DTPA, entered cells after NIR light irradiation

In order to investigate the uptake of molecules after NIR light irradiation, the uptake of ^{111}In-DTPA was studied. The calculated

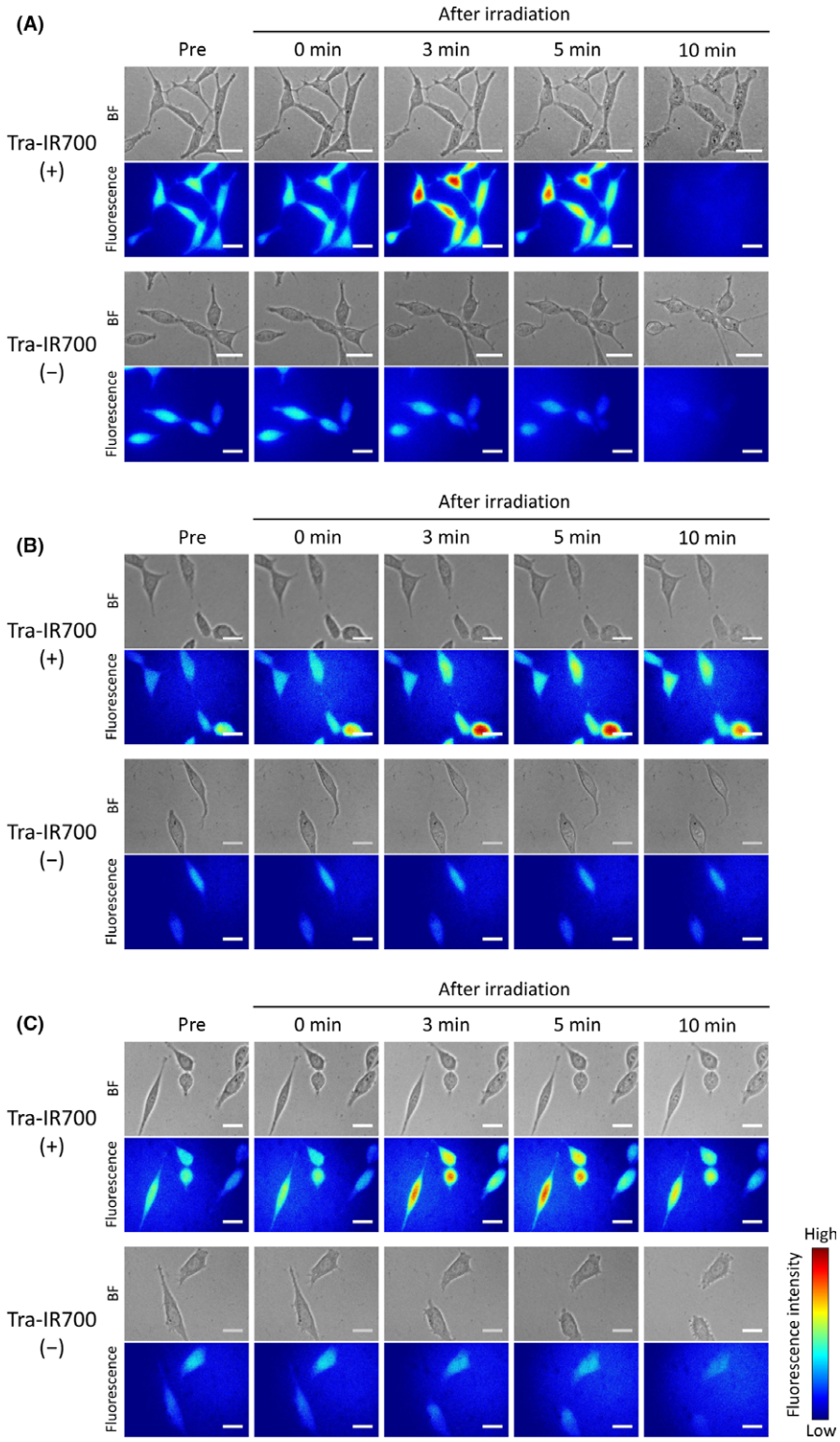

FIGURE 1 Na^+-inflow after near-infrared (NIR) light irradiation. Bright field (BF) and CoroNa Green fluorescence images of Tra-IR700 (+) (top) and Tra-IR700 (–) (bottom) groups. Na^+ entered cells after NIR light irradiation only in the Tra-IR700 (+) group. Na^+-inflow (A) at 37°C, (B) at 4°C, and (C) in the presence of tetrodotoxin (TTX). Scale bar, 20 μm

molecular diameter of ^{111}In-DTPA is approximately 1 nm.[15,16] In a normal medium and in a high osmotic pressure medium established by NaCl, ^{111}In-DTPA did not enter cells at 3 minutes after light exposure, but it eventually flowed into the cells at 60 minutes (Figure 4B). These results supported the notion that plasma membrane permeability increased with time after NIR light irradiation. In

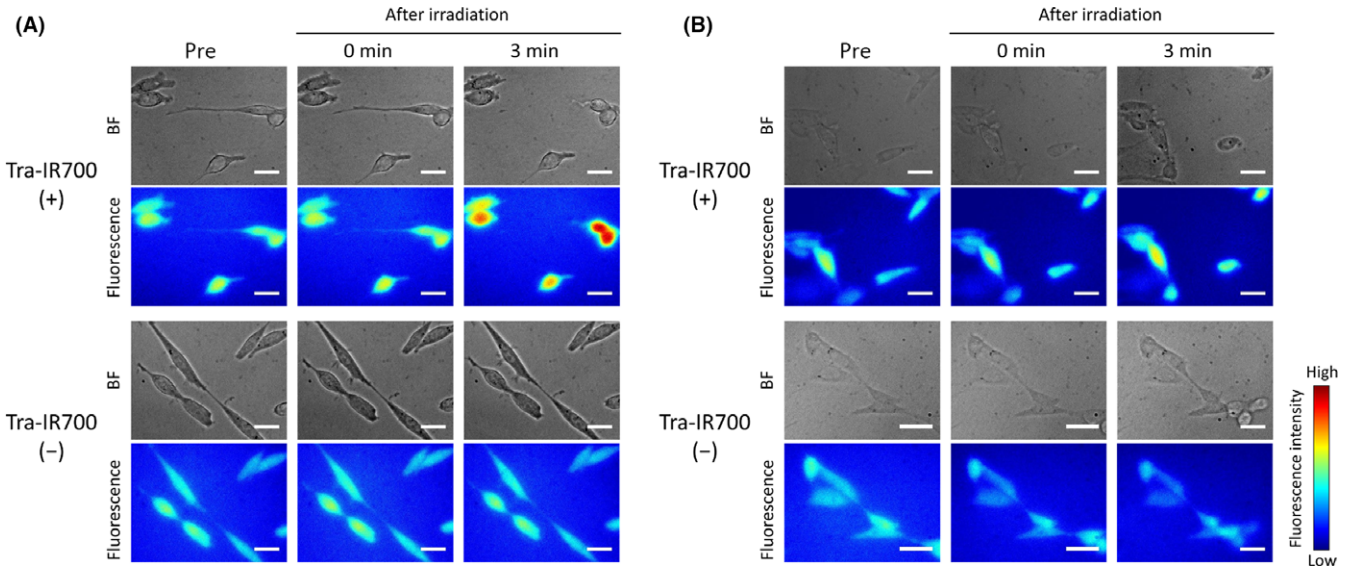

FIGURE 2 Na^+-inflow under high osmotic pressure conditions after near-infrared (NIR) light irradiation. Bright field and CoroNa Green fluorescence images of Tra-IR700 (+) (top) and Tra-IR700 (–) (bottom) groups. A, Na^+-inflow under high osmotic pressure conditions established by NaCl. Na^+ entered cells after NIR light irradiation in the Tra-IR700 (+) group. B, Na^+-inflow under high osmotic pressure conditions established by dextran. Na^+ did not enter cells after NIR light irradiation. Scale bar, 20 μm

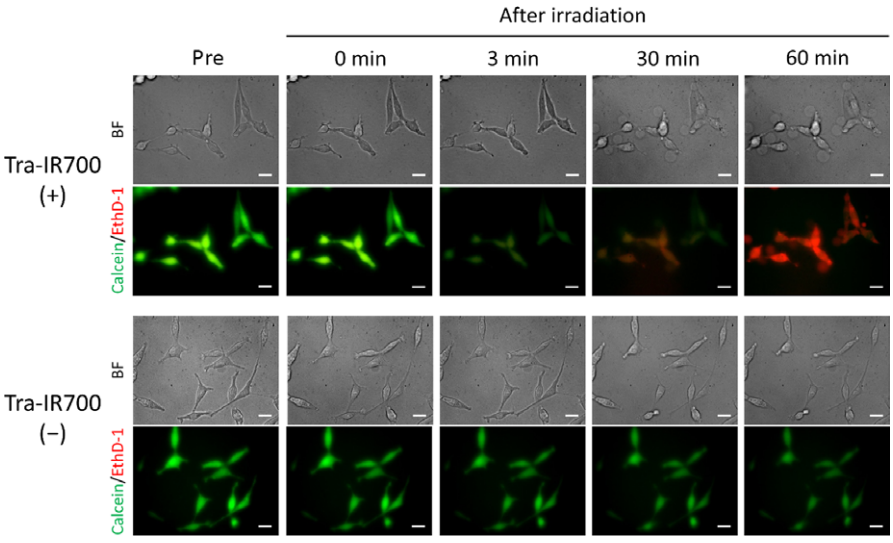

FIGURE 3 Changes in plasma membrane permeability after near-infrared (NIR) light irradiation. Bright field images and calcein and ethidium homodimer-1 (EthD-1) fluorescence images of Tra-IR700 (+) (top) and Tra-IR700 (–) (bottom) groups. In the Tra-IR700 (+) group, calcein leaked out at 3 minutes after NIR light irradiation, and EthD-1 entered cells after many blebs were observed in bright field. In contrast, the fluorescence intensity of calcein decreased as a result of photobleaching and EthD-1 did not enter cells after NIR light irradiation in the Tra-IR700 (–) group. Scale bar, 20 μm

contrast, under high osmotic pressure conditions established by dextran, there was no difference between the Tra-IR700 (+) and Tra-IR700 (–) groups at 3 minutes or at 60 minutes.

3.5 | ^3H-H_2O immediately flowed into cells after NIR light irradiation

Inflow of water molecules after NIR light irradiation was quantified using ^3H-H_2O. As shown in Figure 4C, the Tra-IR700 (+) group showed an increase in uptake in a normal medium and in a high osmotic pressure medium established by NaCl at both 3 and 60 minutes after NIR light irradiation, although it was not statistically significant. In contrast, there was no difference between the Tra-IR700 (+) and Tra-IR700 (–) groups in a high osmotic pressure medium established by dextran. These results indicated that the inflow of water molecules could contribute to the cell swelling observed in NIR-PIT-treated cells.

4 | DISCUSSION

It has been shown previously that cells treated with NIR-PIT underwent cell swelling, bleb formation, and cell membrane rupture,[1,2] which finally resulted in necrotic/immunogenic cell death.[7] In the present study, we investigated changes in plasma membrane damage by observing the permeability for various ions and molecules at an

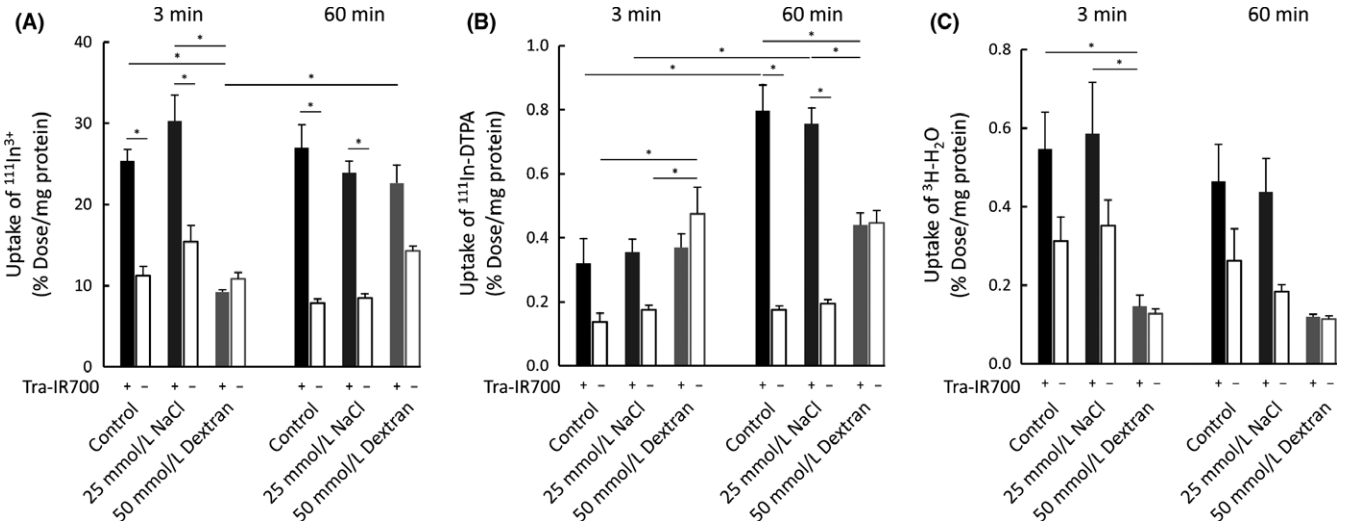

FIGURE 4 Quantitative cell uptake studies of (A) $^{111}In^{3+}$, (B) ^{111}In-DTPA, and (C) ^{3}H-H_2O. A, near-infrared photoimmunotherapy (NIR-PIT)-treated cells in a control and in a high osmotic pressure medium established by NaCl demonstrated the inflow of $^{111}In^{3+}$ at both 3 and 60 min after NIR light exposure. Under high osmotic pressure conditions established by dextran, $^{111}In^{3+}$-inflow was not observed. B, NIR-PIT-treated cells in a control and in a high osmotic pressure medium established by NaCl did not demonstrate the inflow of ^{111}In-DTPA at 3 min, but ^{111}In-DTPA flowed into the cells at 60 min. Under the high osmotic pressure conditions established by dextran, there was no difference between the Tra-IR700 (+) and Tra-IR700 (−) groups neither at 3 min nor at 60 min. C, The Tra-IR700 (+) group showed an increase in uptake in both a normal medium and in a high osmotic pressure medium established by NaCl at both 3 and 60 min after NIR light irradiation, although it was not statistically significant. Data are represented as mean ± SEM (n = 4). Statistical significance was determined by the Tukey-Kramer test (*$P < .05$)

early time point during NIR-PIT. As shown in Figures 1 and 2, it was suggested that minute plasma membrane perforations that were large enough for ions but not for dextran to pass through were induced by NIR-PIT before obvious morphological damage, such as cell swelling, was apparent. Na^+-inflow was observed even when the function of Na^+ transporters or channels was blocked (Figure 1B,C), suggesting that Na^+ was able to penetrate a damaged plasma membrane. Fluorescent intensity was decreased at 10 minutes in Tra-IR700 (+). This can be explained by the leakage of Na^+-indicator itself through the severely damaged plasma membrane. Fluorescent intensity was also decreased at 4°C and in the presence of tetrodotoxin for 10 minutes, but the extent was smaller. This is in accordance with the observation that the membrane damage was smaller in these conditions in 10 minutes. Subsequently, calcein (~1.4 nm) penetrated the damaged plasma membrane, and the larger EthD-1 (~2.6 nm) entered cells after bleb formation (Figure 3). These results suggested that plasma membrane permeability was increased with time after NIR light irradiation. We presume that the plasma membrane damage consists of a tiny "hole" induced by activated mAb-IR700 immediately after NIR light irradiation and that this "hole" is extended with time.

Quantitative cell uptake studies using $^{111}In^{3+}$ and ^{111}In-DTPA supported the above discussion. $^{111}In^{3+}$ uptake was increased both at 3 and 60 minutes after NIR light irradiation (Figure 4A), whereas ^{111}In-DTPA uptake was increased only at 60 minutes (Figure 4B). These results suggested that NIR-PIT induced minute plasma membrane perforations that were large enough for $^{111}In^{3+}$ to pass through immediately after NIR light irradiation, and that plasma membrane permeability was increased with time, which then allowed ^{111}In-DTPA to pass through. Under high osmotic pressure conditions established by dextran, $^{111}In^{3+}$ uptake in Tra-IR700 (+) at 60 minutes was higher than that at 3 minutes, suggesting that the plasma membrane damage became so extensive that even the large dextran molecules could pass through (~3.7 nm). In contrast, there was no difference between ^{111}In-DTPA uptakes at 3 and 60 minutes under high osmotic pressure conditions established by dextran. A possible reason for this "no-difference" may be that ^{111}In-DTPA interacted with dextran, therefore decreasing the diffusion velocity and increasing the time required for ^{111}In-DTPA to enter the cells. Moreover, as dextran is taken up by the cells by endocytosis or absorption through the plasma membrane,[20-22] the uptake of ^{111}In-DTPA attached to dextran might be increased in the Tra-IR700 (−) group under the high osmotic pressure condition established by dextran compared to other osmotic pressure conditions. However, we presume other reasons, such as adsorption to the plasma membrane for the increased uptake of ^{111}In-DTPA, because the uptake was not enhanced in 60 minutes compared to 3 minutes. If it is endocytosis, uptake should be increased with time. In the case of a small-sized molecule, it is not easy for it to be internalized into the cell by endocytosis after adsorption of the molecule to the plasma membrane.[20] The dextran we used in the present study was not large enough for endocytosis (MW ~6000). Thus, we consider that ^{111}In-DTPA-dextran complex was adsorbed to the plasma membrane, but internalization rarely occurred thereafter. Taken together, our results suggested that NIR-PIT initially induced minute plasma membrane perforations that were large enough for small ions to pass through, and that the damage was irreversibly extended with time.

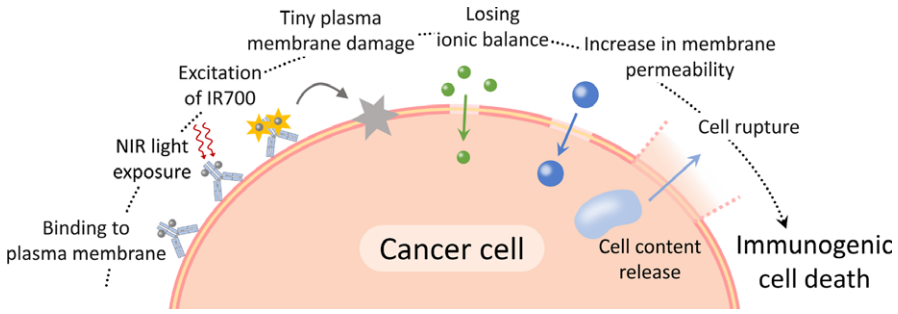

FIGURE 5 A Scheme explaining the changes in plasma membrane damage induced by near-infrared photoimmunotherapy (NIR-PIT)

As cells have a plasma membrane repair mechanism that responds to damage in order to prevent cell death,[23,24] tiny plasma membrane perforations usually do not induce cell death (eg, electroporation[25] and bead-loading[26]). In contrast, the minute damage induced by NIR-PIT was irreversibly extended, and the permeability was increased without membrane repair. It is possible that the permeability increase is partly related to breakdown of cytoskeletal proteins such as actin,[27] as the inflow of Ca^{2+} can activate cysteine proteases, which affect the plasma membrane through proteolysis of cytoskeletal proteins.[28] The ion-inflow also disturbs the intracellular ionic balance and induces water inflow, followed by cell swelling.[29,30] In fact, in our experiments, Figure 4C indicated that water molecules (^3H-H_2O) entered cells after NIR light irradiation and that the inflow of water molecules was prevented in high osmotic pressure conditions. Although further in vivo studies are needed by local injection of dextran, high osmolality might function to be temporally protective to this cell death. Therefore, the minute plasma membrane perforations, through which ions can pass, would be a trigger for the permeability increase, plasma membrane rupture, and necrotic/immunogenic cell death during NIR-PIT (Figure 5).

We demonstrated that the minute plasma membrane perforations induced by mAb-IR700 of NIR-PIT have different characteristics in terms of the passage of ions and molecules, compared to membrane-targeted photosensitizers of PDT. That is, potassium ion and calcein do not pass thorough the plasma membrane after conventional membrane-targeted PDT.[31] In contrast, our results showed that sodium ion and calcein passed through the damaged plasma membrane induced by NIR-PIT. Thus, although similar membrane damage seems to be induced by both phototherapies, membrane permeability for ions and molecules after irradiation was clearly different, suggesting that the mechanism causing the membrane damage should be different. Membrane lipid peroxidation is responsible for inducing membrane damage in PDT,[32,33] but any oxidative changes on major unsaturated lipid molecules after NIR-PIT have not been detected so far.[5,12] Unlike conventional plasma membrane-targeted photosensitizers, an mAb-IR700 is sufficiently far away from the plasma membrane and does not induce oxidative damage because of the very short half-life of singlet oxygen.[12,34] There is a report that free radical scavengers reduced the effect of NIR-PIT,[35] although this has not been generally accepted.[5,11]

The molecular mechanism causing such minute plasma membrane damage in NIR-PIT remains unclear. As the membrane damage is not mainly caused by ROS generation,[1,5] further research on IR700 after NIR light irradiation seems to be needed in order to fully understand the mechanism of NIR-PIT. However, our findings provide new information regarding the cytotoxic damage of the plasma membrane at early time points during NIR-PIT. This study indicated that irreversible minute damage on the plasma membrane was induced before significant morphological damage became apparent, which should be important for NIR-PIT.

ACKNOWLEDGMENTS

This work was supported by PRESTO (JPMJPR15P5), Japan Science and Technology Agency, JSPS KAKENHI Grant Numbers 16H05382 and 16K15568, Astellas Foundation for Research on Metabolic Disorders, and TERUMO Foundation for Life Sciences and Arts.

CONFLICTS OF INTEREST

Authors declare no conflicts of interest for this article.

ORCID

Mikako Ogawa http://orcid.org/0000-0002-3432-4519

REFERENCES

1. Mitsunaga M, Ogawa M, Kosaka N, Rosenblum LT, Choyke PL, Kobayashi H. Cancer cell–selective in vivo near infrared photoimmunotherapy targeting specific membrane molecules. *Nat Med*. 2011;17:1685-1691.
2. Ogata F, Nagaya T, Okuyama S, et al. Dynamic changes in the cell membrane on three dimensional low coherent quantitative phase microscopy (3D LC-QPM) after treatment with the near infrared photoimmunotherapy. *Oncotarget*. 2017;8:104295-104302.
3. Dougherty TJ, Gomer CJ, Henderson BW, et al. Photodynamic therapy. *J Natl Cancer Inst*. 1998;90:889-905.
4. Agostinis P, Berg K, Cengel KA, et al. Photodynamic therapy of cancer: an update. *Am Cancer Soc*. 2011;61:250-281.
5. Shirasu N, Yamada H, Shibaguchi H, Kuroki M, Kuroki M. Potent and specific antitumor effect of CEA-targeted photoimmunotherapy. *Int J Cancer*. 2014;135:2697-2710.

6. Ito K, Mitsunaga M, Arihiro S, et al. Molecular targeted photoimmunotherapy for HER2-positive human gastric cancer in combination with chemotherapy results in improved treatment outcomes through different cytotoxic mechanisms. *BMC Cancer*. 2016;16:1-10.
7. Ogawa M, Tomita Y, Nakamura Y, et al. Immunogenic cancer cell death selectively induced by near infrared photoimmunotherapy initiates host tumor immunity. *Oncotarget*. 2017;8:10425-10436.
8. Nakamura Y, Nagaya T, Sato K, et al. Alterations of filopodia by near infrared photoimmunotherapy: evaluation with 3D low-coherent quantitative phase microscopy. *Biomed Opt Express*. 2016;7:2738-2748.
9. Moan J, Pettersen EO, Christensen T. The mechanism of photodynamic inactivation of human cells in vitro in the presence of haematoporphyrin. *Br J Cancer*. 1979;39:398-407.
10. Kim J, Santos OA, Park JH. Selective photosensitizer delivery into plasma membrane for effective photodynamic therapy. *J Control Release*. 2014;191:98-104.
11. Jin J, Krishnamachary B, Mironchik Y, Kobayashi H, Bhujwalla ZM. Phototheranostics of CD44-positive cell populations in triple negative breast cancer. *Sci Rep*. 2016;6:27871.
12. Railkar R, Krane LS, Li QQ, et al. Epidermal growth factor receptor (EGFR) targeted photoimmunotherapy (PIT) for the treatment of EGFR expressing bladder cancer. *Mol Cancer Ther*. 2017;16:2201-2214.
13. Meier SD, Kovalchuk Y, Rose CR. Properties of the new fluorescent Na^+ indicator CoroNa Green: comparison with SBFI and confocal Na^+ imaging. *J Neurosci Methods*. 2006;155:251-259.
14. Goldin AL. Resurgence of sodium channel research. *Annu Rev Physiol*. 2001;63:871-894.
15. Lu X, Nguyen V, Zeng X, Elliott BJ, Gin DL. Selective rejection of a water-soluble nerve agent stimulant using a nanoporous lyotropic liquid crystal-butyl rubber vapor barrier material: evidence for a molecular size-discrimination mechanism. *J Memb Sci*. 2008;318:397-404.
16. Baransi K, Dubowski Y, Sabbah I. Synergetic effect between photocatalytic degradation and adsorption processes on the removal of phenolic compounds from olive mill wastewater. *Water Res*. 2012;46:789-798.
17. Marcus Y. Ionic radii in aqueous solutions. *Chem Rev*. 1988;88:1475-1498.
18. Iamshanova O, Mariot P, Lehen'kyi V, Prevarskaya N. Comparison of fluorescence probes for intracellular sodium imaging in prostate cancer cell lines. *Eur Biophys J*. 2016;45:765-777.
19. Venturoli D, Rippe B. Ficoll and dextran vs. globular proteins as probes for testing glomerular permselectivity: effects of molecular size, shape, charge, and deformability. *Am J Physiol Renal Physiol*. 2005;288:F605-F613.
20. Al Soraj M, He L, Peynshaert K, et al. siRNA and pharmacological inhibition of endocytic pathways to characterize the differential role of macropinocytosis and the actin cytoskeleton on cellular uptake of dextran and cationic cell penetrating peptides octaarginine (R8) and HIV-Tat. *J Control Release*. 2012;161:132-141.
21. Mains PE, Sulston IA, Wood WB. Dominant maternal-effect mutations causing embryonic lethality in *Caenorhabditis elegans*. *Genetics*. 1990;125:351-369.
22. Lei L, Tao W, Min W, Bei L, Ran C, Rongying Z. The effect of the size of fluorescent dextran on its endocytic pathway. *Cell Biol Int*. 2015;39:531-539.
23. Andrews NW, Almeida PE, Corrotte M. Damage control: cellular mechanisms of plasma membrane repair. *Trends Cell Biol*. 2014;24:734-742.
24. Blazek AD, Paleo BJ, Weisleder N. Plasma membrane repair: a central process for maintaining cellular homeostasis. *Physiology*. 2015;30:438-448.
25. Neumann E, Schaefer-Ridder M, Wang Y, Hofschneider PH. Gene transfer into mouse lyoma cells by electroporation in high electric fields. *EMBO J*. 1982;1:841-845.
26. McNeil PL, Warder E. Glass beads load macromolecules into living cells. *J Cell Sci*. 1987;88(Pt 5):669-678.
27. Liu X, Van Vleet T, Schnellmann RG. The role of calpain in oncotic cell death. *Annu Rev Pharmacol Toxicol*. 2004;44:349-370.
28. Fink SL, Cookson BT, Fink SL, Cookson BT. Apoptosis, pyroptosis, and necrosis: mechanistic description of dead and dying eukaryotic cells. *Infect Immun*. 2005;73:1907-1916.
29. Trump BF, Berezesky IK. The role of altered $[Ca^{2+}]i$ regulation in apoptosis, oncosis, and necrosis. *Biochim Biophys Acta*. 1995;1313:173-178.
30. Okada Y, Sato K, Numata T. Pathophysiology and puzzles of the volume-sensitive outwardly rectifying anion channel. *J Physiol*. 2009;587:2141-2149.
31. Kotova EA, Kuzevanov AV, Pashkovskaya AA, Antonenko YN. Selective permeabilization of lipid membranes by photodynamic action via formation of hydrophobic defects or pre-pores. *Biochim Biophys Acta*. 2011;1808:2252-2257.
32. Girotti AW. Photodynamic lipid peroxidation in biological systems. *Photochem Photobiol*. 1990;51:497-509.
33. Thomas JP, Girotti AW. Role of lipid peroxidation in hematoporphyrin derivative-sensitized photokilling of tumor cells: protective effects of glutathione peroxidase. *Cancer Res*. 1989;49:1682-1686.
34. Moan J, Berg K. The photodegradation of porphyrins in cells can be used to estimate the lifetime of singlet oxygen. *Photochem Photobiol*. 1991;53:549-553.
35. Kishimoto S, Bernardo M, Saito K, et al. Evaluation of oxygen dependence on in vitro and in vivo cytotoxicity of photoimmunotherapy using IR-700-antibody conjugates. *Free Radic Biol Med*. 2015;85:24-32.

SUPPORTING INFORMATION

Additional supporting information may be found online in the Supporting Information section at the end of the article.

How to cite this article: Nakajima K, Takakura H, Shimizu Y, Ogawa M. Changes in plasma membrane damage inducing cell death after treatment with near-infrared photoimmunotherapy. *Cancer Sci*. 2018;109:2889–2896. https://doi.org/10.1111/cas.13713